International Journal of Bioelectromagnetism
Vol. 22, No. 1, pp. 20 - 24, 2020

www.ijbem.org

Chirp Transform in Bioimpedance Spectroscopy

Olev Märtens[a], Mart Min[a], Raul Land, Jaan Ojarand[a], and Paul Annus[a]

[a]Thomas Johann Seebeck Department of Electronics, Tallinn University of Technology, Estonia

Correspondence: M.Min, Thomas Johann Seebeck Department of Electronics, School of Information Technology Tallinn University of Technology, Ehitajate tee, 19086 Tallinn, Estonia, EU

mart.min@taltech.ee

Abstract. The impedance spectrum of dynamic systems is time-dependent. Fast impedance changes take place, e.g., in living cardiovascular and pulmonary systems. Measurements must be as short as possible to avoid significant impedance changes during the spectral analysis, and as long as possible to enlarge the excitation energy for obtaining the highest signal-to-noise ratio (SNR). The authors propose to use chirp waveforms for excitation (perturbation) signals thanks to their scalability. Separate and almost independent scalability of chirps both in time and frequency domains gave us a possibility to find the best compromise between the controversial requirements between spectral bandwidth, measurement time, and allowed SNR. The chirp wave excitation can include thousands of cycles when the impedance changes are slow. However, it can contain only some cycles, also a single cycle or even a part of it, if the speed of impedance variations is very high. The excitation bandwidth is maintained at the expense of the reduction in excitation energy. The authors show how to generate the chirps with different duration but the same bandwidth up to some MHz and how to use these signals in the time-dependent impedance spectroscopy.

Keywords: ECG, ICG, dynamic impedance, impedance spectroscopy, excitation, synchronization, chirp transform

1. Introduction

Bioimpedance spectroscopy enables one to characterize time-varying biological matter when the measurement speed is high enough (Sanchez et al., 2015). The bioimpedance spectroscopy can serve as a diagnosing method, based on spectral snapshots of the impedance of beating heart or pulsating cardiovascular system and respiratory tract (Min et al., 2007; Sanchez et al., 2015) for obtaining cycle-by-cycle impedance spectrograms. Short broadband excitation and fast processing of the response signal are both important to achieve the required speed of spectral analysis (Min et al., 2011, 2014). Different signal waveforms are used (Chang et al., 2016; Min et al., 2007, 2011, 2014; Sanchez et al., 2015). The chirp wave assumed favorable in many cases because of its inherent scalability, both in time and frequency (Mann and Haykin, 1995; Min et al., 2007, 2014).

For getting the best results, first, we must minimize the measurement time to restrict the dynamic uncertainties caused by impedance changes during the measurement process. At the same time, we must prolong the measurement time as much as possible in order to enhance the signal-to-noise ratio (SNR) by smoothing out the background noise. Remark: The possibility to enhance the SNR by enlarging the excitation amplitude is very limited because of the constraints applied to electrical currents in the human body, e.g., from 10 μA in case of invasive measurements at low frequencies, and up to some mA, when measuring non-invasively at higher frequencies. The optimal solution is a balanced trade-off between the speed of impedance variations, measurement time, and excitation bandwidth. A key factor in finding a successful compromise is the independent scalability in time (duration of measurement) and frequency (measurement bandwidth), both available when using chirp signals (Min et al., 2011). Low-cost field-programmable gate array (FPGA) chips (Trebbels et al., 2012) are suitable to generate chirp signals with controllable parameters. Carefully synchronized correlation of the response to the applied excitation with sine-chirp and cosine-chirp reference signals (Märtens et al., 2014) enables the development of effective devices for the simultaneous time-frequency measurement and analysis of time-varying impedances.

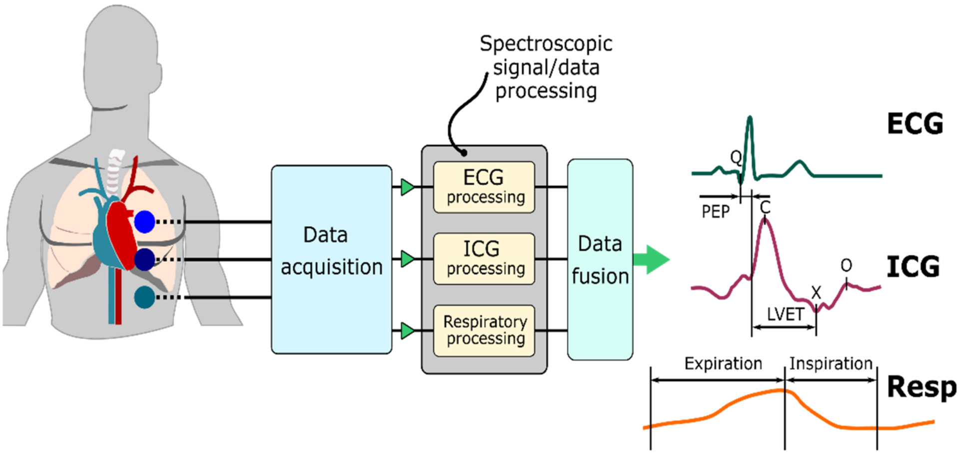

Figure 1. *A draft of the device for time-frequency domain analysis of cardio-pulmonary parameters: ECG – electrocardiogram, ICG – impedance cardiogram, Resp – respiratory impedance curve.*

2. From sine wave to implementation of chirp waveforms

2.1 Sine wave and chirp

Oliver Heaviside coined the term impedance in 1886, and Arthur Kennelly introduced the complex numbers in 1893 for characterization of electrical impedance (Brattain, 2006) on a sine wave basis. The sine wave is a function $A\sin[\Phi(t)]$ of linearly growing phase $\Phi(t) = \int \omega\, dt = \omega t$ with constant angular frequency $d[\Phi(t)]/dt = \omega$, rad/s.

Chirp waveform also expresses by sine and cosine, but its definition is much broader. The angular frequency $\omega(t)$ of chirp can change arbitrarily in time t, and because of that, the frequency $\omega(t_i)$ is called the instantaneous angular frequency at the moment t_i. When controlling angular frequency $\omega(t)$, we cannot determine the chirp, because we do not know the value of running phase $\Phi(t)$ at every moment t_i. We know only angular frequency $\omega(t)$ with some error $\delta[\omega(t)]$, which can be negligibly small but is always existing. The phase error $\delta(\Phi(t)) = \int \delta(\omega(t))dt$ is a cumulatively growing function (integral) and the signals with controllable frequency but unknown phase are sweeps, not chirps.

Fortunately, nowadays, devices for direct digital synthesis (DDS) enable to control the phase directly and continuously (Trebbels et al., 2012; Min et al., 2011). Direct phase control ensures continuity of sine wave chirps and makes possible the use of chirps in the measurement of time-varying impedances (Trebbels et al., 2012; Sanchez et al., 2012; Märtens et al., 2014; Min et al., 2014).

2.2 Sine wave linear chirps

In general, a linear sine wave chirp $\mathrm{sinChirp}(t) = A\sin\Phi(t)$ can be described as

$$A\sin\left[\int \omega(t)dt + \Phi\right] = A\cdot\sin[2\pi(f_1\cdot t + B\cdot t^2/2T)] \qquad (1)$$

with constantly growing angular frequency ($\omega(t) = \omega t = 2\pi f\cdot t$) and zero value initial phase ($\Phi = 0$), where f_1 and f_2 the are the initial and final frequencies, defining the bandwidth $B = f_2 - f_1$, which is covered with a chirping rate $K = B/T$ during the existence T of the chirp. The parameters, as root-mean-square value $RMS = A/\sqrt{2} = 0.707A$ and crest factor $CF = A/RMS = \sqrt{2}$ remain the same as for sinusoidal signal, also the energy $E = (A^2/2)\cdot T$ depends linearly on the signal duration T.

<u>Example:</u> Taking f_1 =10 kHz, f_2 =1MHz, and T = 1ms for our experiments, the chirp covers the bandwidth $B = f_2 - f_1$ = 990 kHz with chirping rate K = B /T = 990 kHz/ms = $9.9\cdot10^8$ Hz/s. Number of full cycles P (Min *et al.*, 2011) is equal to $T(f_1 + f_2)/2 = 505$.

2.3 Generation of signals for chirplet transform

For the measurement impedance variations, we synthesize a normalized excitation signal $1\mathrm{sinChirp}(t_i)$, see Fig. 3, synchronously with the normalized reference chirps $1\mathrm{sinChirp}(t_i)$ and $1\mathrm{cosChirp}(t_i)$ under the common clock operating non-uniformly in time (Fig. 2). The same clock works uniformly for the discrete-time synthesizing of the chirp waveforms sampling after every 10 degrees within the full chirp cycle covering 360 degrees, see Fig.2. Applying the excitation chirp (Fig. 3) to the measured impedance, we receive the response signal, with which the correlation with normalized sin/cos reference chirps (Fig. 2) is performed (Mann and Haykin, 1995; Märtens et al., 2014; Chang et al., 2016). After performing the correlation procedure (the chirplet transform), the extracted impedance variations become available both in time and frequency domain (Fig. 4 and Fig. 5).

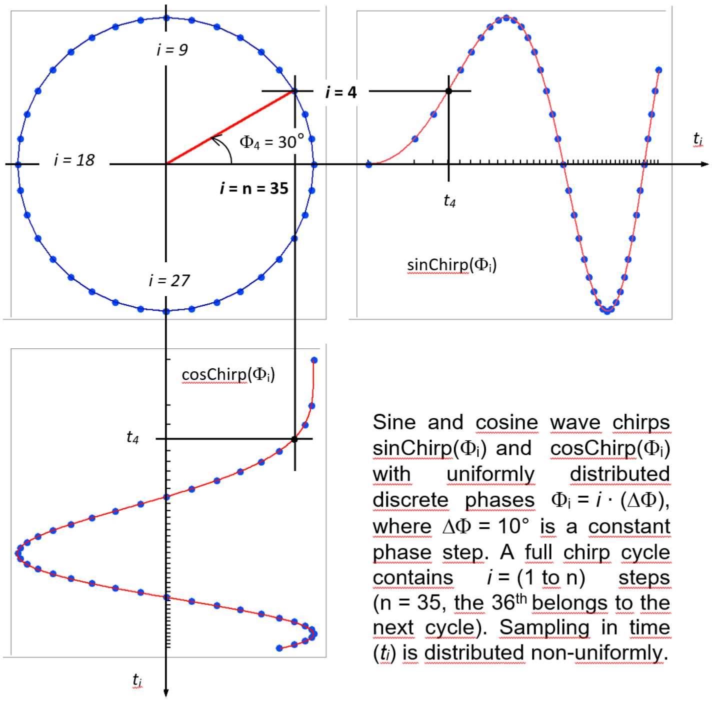

Figure 2. *Discrete-time formation of sinChirp(t_i) and cosChirp(t_i) for chirplet transform.*

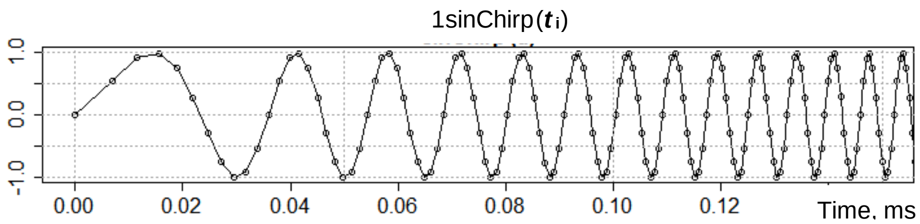

Figure 3. *The initial section of the excitation signal sinChirp(t_i) formed at non-uniformly distributed moments.*

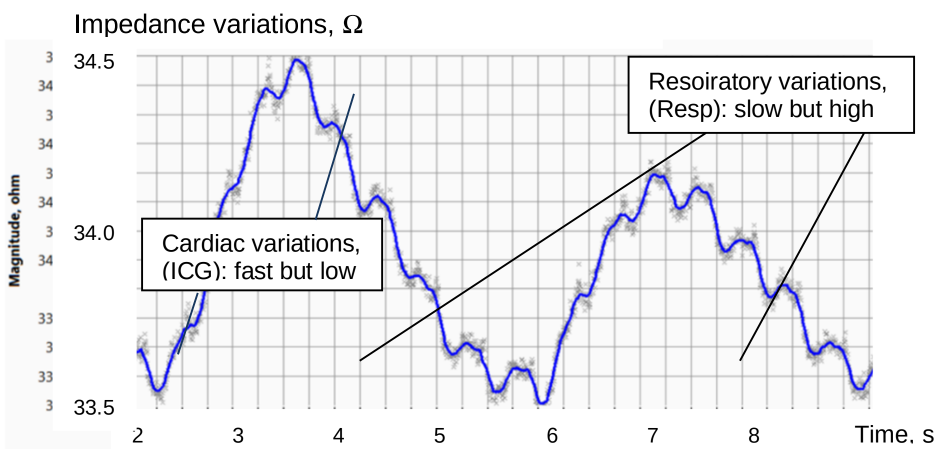

Figure 4. *Respiratory (Resp) and cardiac (ICG) variations demodulated from the response signal.*

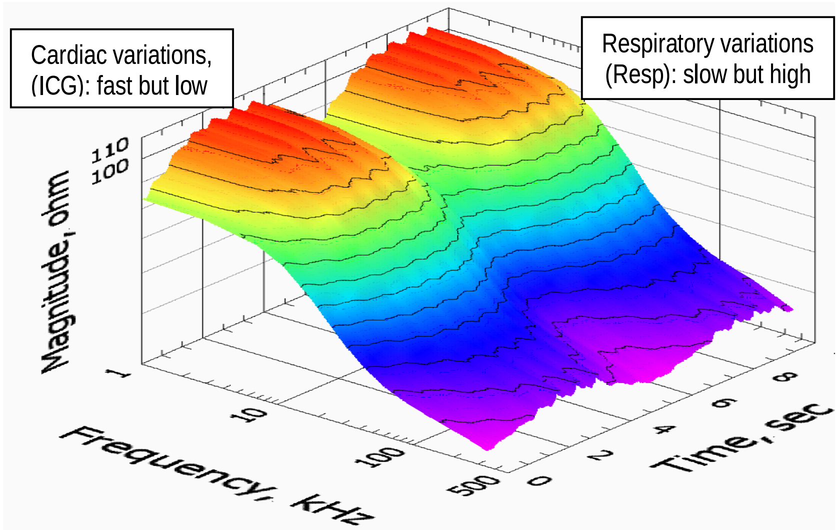

Figure 5. *Spectrogram of the ICG and Resp variations presented simultaneously in the time-frequency domain.*

3. Conclusions

The Chirp Transform enables us to perform the time-limited analysis of bioimpedance variations of our body compartments and organs simultaneously, both in time and frequency domain. Thanks to the scalability of chirp functions, we can find a trade-off between the speed of impedance variations, measurement time, required frequency bandwidth, and, finally, taking into account the demand for signal-to-noise ratio (SNR). For example, a 100 kHz bandwidth can be covered by the chirp signal, which lasts as short as 10 μs or as long as 1s (difference in 100 thousand times), also allowing the excitation energy differ in 10^5 times, which makes 316 times in root-mean-square (RMS) value and the same in SNR.

The developed low complexity and low computing power demanding algorithms enable us to design simpler and less electric power consuming impedance spectroscopy devices than those using fast Fourier (FFT), and short-time Fourier transforms (STFT) for similar tasks. Using hardware MAC (multiply and accumulate) units for single-instruction multiplications needs only N operations (FFT needs $N \cdot \log_2 N$ multiplications, N is a number of samples). The power consumption lowers proportionally to operations.

Acknowledgments

The work has been supported by the Estonian Research Council and EU Regional Fund (projects EAG34, EXCITE, FLAG-ERA-JTC-Call 2016-CONVERGENCE, and CHIST-ERA-Call 2018-JEDAI).

References

Brittain JE. (2006). Electrical Engineering Hall of Fame: Arthur Kennelly. *Proc. IEEE*. 94(9): pp. 1772–5.

Chang X., Cong W., & Jingbo G. (2016). Instantaneous Frequency Identification Using Adaptive Linear Chirplet Transform and Matching Pursuit Shock and Vibration (Acad. Ed. E. Mucchi), ID 1762010 (10 pp). Retrieved from: *http://dx.doi.org/10.1155/2016/1762010*

Mann S. & Haykin S. (1995). The chirplet transform: physical considerations. *IEEE Trans. Sign. Proc*. 43(11): pp. 2745 – 61.

Min M., Pliquett U., Nacke T., Barthel A., Annus P., & Land R. (2007). Signals in bioimpedance measurement: different waveforms for different tasks. *IFMBE Proc. 17 (13th Int. Conf. on Electrical Bioimpedance ICEBI'2007)*, Graz, Austria, Aug 29–Sept 2, 2007): pp. 181 – 4. Retrieved from: https://link.springer.com/chapter/10.1007/978-3-540-73841-1_49

Min M., Land R., Paavle T., Parve T., Annus P., & Trebbels D (2011). Broadband Spectroscopy of Dynamic Impedances with Short Chirp Pulses. *Phys.Meas.* 32(7): pp. 945-958. https://iopscience.iop.org/article/10.1088/0967-3334/32/7/S16/meta

Min M., Paavle T., Land R., Annus P., & Parve T. (2014). *Method and Device for Fast Measurement of Frequency Response with Scalable Short Chirp Signals.* US Patent 8,674,680 B2. Retrieved from: https://patents.google.com/patent/US8854030

Märtens O., Min M., Land R., Annus P., Saar T. & Reidla M. (2014). *Method and Device for Frequency Response Measurement.* US Patent 8,854,030 B2. Retrieved from: https://patents.google.com/patent/US8854030

Sanchez B., Louarroudi E., Pintelon R. (2015). Time-invariant measurement of time-varying bioimpedance using vector impedance analysis. *Physiol. Meas*. 36(3): pp. 595-620. Retrieved from: https://iopscience.iop.org/article/10.1088/0967-3334/36/3/595/meta

Trebbels D., Fellhauer F., Jugl M., Haimerl, G., Min M., & Zengerle R. (2012). OnlineTissue Discrimination for Transcutaneous Needle Guidance Applications Using Broadband Impedance Spectroscopy. *IEEE Trans. Biomed. Eng*. 59(2): pp. 494-503.